inter.noise
HAMBURG 2016

Sound Absorption Measurements: Comparison of Standard Tests in Reverberant Room with Measurements using a Synthetized Diffuse Acoustic Field

O. Robin*[1], C.K. Amedin*[2], A. Berry*[3], N. Atalla*[4], O. Doutres#[5] and F. Sgard+[6]

* Groupe d'Acoustique de l'Université de Sherbrooke
Faculté de Génie, Sherbrooke, J1K 2R1, Canada.
Ecole de Technologie Supérieure de Montréal
1100 Rue Notre-Dame O., Montréal, H3C 1K3, Canada.
+ Institut de Recherche Robert Sauvé en Santé et Sécurité du Travail
505 Boulevard de Maisonneuve O., Montréal, H3A 3C2, Canada.

ABSTRACT

This communication mainly aims at providing a comprehensive comparison of measurements of sound absorption coefficients performed following standard in a reverberant room and using a synthetized Diffuse Acoustic Field. Using sound field reproduction approaches and a synthetic array of acoustic monopoles facing a material, estimation of the sound absorption coefficient under a reproduced Diffuse Acoustic Field in a hemi-anechoic room was previously shown to be feasible.

Five different acoustic materials are tested. Melamine foam is used as a reference case, while the other four are utilized in the building industry: fiberglass batts, heavy-density fiberglass boards, polyurethane foam and ceiling tiles. Results obtained following standards, a synthetized diffuse field and also theoretical predictions assuming materials of infinite extent are compared.

It is shown that the sound absorbing coefficients under a diffuse acoustic field excitation can be estimated with satisfactory accuracy using the synthetic diffuse field approach. The sample area is significantly reduced compared to standard requirements and a reverberant room is no longer needed. The effect of the source height and of the array source density on obtained results is also briefly investigated using FEM calculations. Possible improvements of the method at low frequency are finally discussed.

Keywords: Sound absorption, reverberant room

PACS numbers: 43.55.Ev

1. INTRODUCTION

This paper reports experimental and simulations results concerning the estimation of sound absorption coefficient using a synthetized Diffuse Acoustic Field (DAF). The effect of the synthetic array size and of the sample size were previously examined in [1, 2]. In this paper, experimental results of sound absorption measurements for five materials using the standardized reverberant room method and the synthetized DAF method using the laboratory setup described in [3] are presented, as well as the effect of the synthetic array height on numerical results.

[1]email: olivier.robin@usherbrooke.ca
[2]email: celse.kafui.amedin@usherbrooke.ca
[3]email: alain.berry@usherbrooke.ca
[4]email: noureddine.atalla@usherbrooke.ca
[5]email: olivier.doutres@etsmtl.ca
[6]email: franck.sgard@irsst.qc.ca

2. THEORY

2.1 Sound absorption in reverberant rooms

Random-incidence sound absorption coefficients, also known as *Sabine absorption coefficients*, are estimated in reverberant chambers following ASTM C423 [4]. Once the reverberation times (in seconds and in third octave bands) with and without a sample (T_{sample} and T_0, respectively) are measured, the absorption coefficient can be calculated following

$$\alpha = \frac{55.3V}{S}\big[\frac{1}{T_{sample}} - \frac{1}{T_0}\big], \tag{1}$$

where V is the reverberation chamber volume and S the sample area (an area of 6.7 m^2, *i.e.* 72 ft^2, is customary).

2.2 Sound absorption under a point source

Under the assumption of an ideal point source positioned at a given position i at a height $z = z_3$ above a layer of porous material, the acoustic field at any of the microphones $M1$ and $M2$ (placed above the porous material at heights $z = z_1$ and $z = z_2$, respectively) is a superposition of two spherical acoustic waves, generated by the source and the corresponding image source (see Fig. 1(a)). For a small separation of the two microphones so that the angle θ_i is almost identical for both microphones, the measured acoustic pressure $\tilde{p}_{ij}(\theta_i, \omega)$ for a given position i of the point source at microphone M_j ($j = 1, 2$) can be written

$$\tilde{p}_{ij}(\theta_i, \omega) = \rho_0 q_i(\omega)\big(\frac{e^{-jk_0 r_{ij}}}{r_{ij}} + R(\theta_i, \omega)\frac{e^{-jk_0 r'_{ij}}}{r'_{ij}}\big), \tag{2}$$

with ρ_0 the air mass density, ω the angular frequency, k_0 the acoustic wavenumber ($k_0 = \omega/c_0$ with c_0 the speed of sound), $q_i(\omega)$ is the source volume acceleration, r_{ij} the distance between the source at the *i*-th position and the microphone M_j, r'_{ij} the distance between the image source and the microphone M_j and $R(\theta_i, \omega)$ is the reflection coefficient of the material surface corresponding to the i-th position of the point source. The measurement of either $\tilde{p}_{ij}(\theta_i, \omega)/q_i(\omega)$ at each microphone or $H(\theta_i, \omega)(= \tilde{p}_{i2}(\theta_i, \omega)/\tilde{p}_{i1}(\theta_i, \omega))$ allows calculating the reflection coefficient for a given incidence angle using the classical relation [5]

$$R(\theta_i, \omega) = \frac{\frac{e^{-jk_0 r_{i2}}}{r_{i2}} - H(\theta_i, \omega)\frac{e^{-jk_0 r_{i1}}}{r_{i1}}}{H(\theta_i, \omega)\frac{e^{-jk_0 r'_{i1}}}{r'_{i1}} - \frac{e^{-jk_0 r'_{i2}}}{r'_{i2}}}. \tag{3}$$

The corresponding absorption coefficient is then deduced using the relation $\alpha(\theta_i, \omega) = 1 - |R(\theta_i, \omega)|^2$.

2.3 Sound absorption under a synthesized pressure field

Figure 1(b) illustrates the proposed approach. A square sample of porous material of sidelength L and thickness h is placed on a rigid impervious backing. The source synthetic array and the two microphones $M1$ and $M2$ are centered on the material's surface. Using the two-microphones method described in the previous section, the reflection coefficient can be measured under various incidence angles corresponding to successive source positions i of point sources, thus creating a virtual array of monopoles in front of the material surface.

The Green's functions corresponding to the propagation from the real (respectively image) point source to the microphone M_j will now be denoted $g_{ij}(\omega) = \frac{e^{-jk_0 r_{ij}}}{r_{ij}}$ (respectively $g'_{ij}(\omega) = \frac{e^{-jk_0 r'_{ij}}}{r'_{ij}}$).

It can be shown (details can be found in [3]) that with a database of measured reflection coefficients $R(\theta_i, \omega)$ for various source positions and a calculated CSD matrix of source volume accelerations S_{QQ} (that when applied to all the virtual sources would lead to the reproduction of a desired pressure field at the material surface), Eq. (4) below provides the squared reflection coefficient $|R_{synth}(\omega)|^2$ under a synthesized pressure field at a post-processing phase :

$$|R_{synth}(\omega)|^2 = \frac{\mathbf{h_1}^H \mathbf{S_{QQ}} \mathbf{h_1}}{\mathbf{g'_1}^H \mathbf{S_{QQ}} \mathbf{g'_1}}, \tag{4}$$

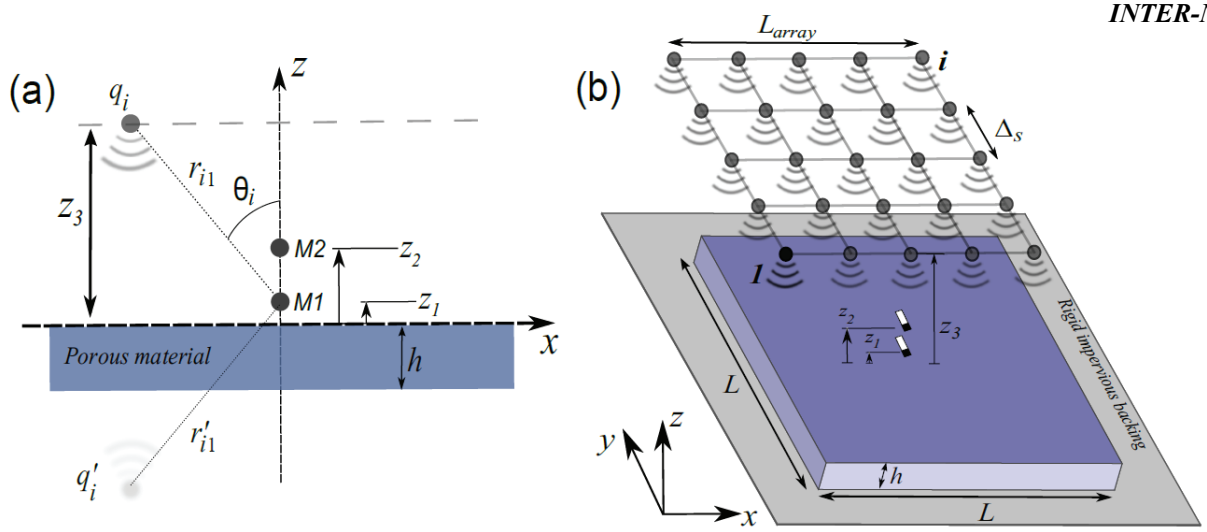

Figure 1: (a) Description of the problem and coordinate system for a spherical wave model using a single point source – (b) Description of the problem using a i-source array (the sidelength of the virtual array is L_{array}, with uniformly distributed sources positioned with the same source separation Δ_s) [From Robin[3]].

where $g'_1 = \{\dots g'_{i1} \dots\}^T$, $h_1 = \{\dots R(\theta_i, \omega) g'_{i1} \dots\}^H$ and ^{T} and ^{H} denote the tranpose and hermitian transpose, respectively. The CSD matrix of source volume acceleration S_{QQ} can be calculated using either a Wave Field Synthesis (WFS) approach [6] or a Planar Nearfield Acoustical Holography (P-NAH) approach [7] (in this paper, the latter is used), with a target pressure field defined by the CSD of an ideal DAF [8]. The corresponding absorption coefficient can be finally deduced using the relation $\alpha_{synth}(\omega) = 1 - |R_{synth}(\omega)|^2$.

Note first that while two microphones are needed for the calculation of the individual reflection coefficients $R(\theta_i, \omega)$ (following the procedure described in previous section), the calculation of the squared reflection coefficient under a synthetic pressure field $|R_{synth}(\omega)|^2$ requires only one microphone position (here microphone $M1$). Also, the squared absolute reflection coefficient used for this calculation is calculated at a specific (or local) position on the material surface, unlike the 'global' absorption result obtained with the reverberant room method.

3. TESTED MATERIALS

Five different materials were considered in the experimental part of this work : (1) melamine foam, (2) fiberglass, (3) high density fiberglass board (HDFB), (4) polyurethane foam (PUF) and (5) ceiling tiles. For modeling purposes using the Johnson-Champoux-Allard (JCA) model [9], the non-acoustic parameters of materials were measured in the Acoustic Materials Characterization Labs of Groupe d'Acoustique de l'Université de Sherbrooke (GAUS), using the methods described in [10] (Direct measurements were also performed for mass density, open porosity [11] and static air flow resisistivity [12]). Obtained parameters for the five materials are given in Table 1. Pictures of samples of 100 mm and 44.5 mm diameters, that were used for impedance tube measurements, are given in figure 2, respectively. Four of the materials had close thicknesses (14.5 mm for tiles, 22 mm for the HDFB tile and 25 mm for both melamine foam and PUF) while the fiberglass thickness reached 80 mm.

4. DESCRIPTION OF MEASUREMENTS AND SIMULATIONS

Reverberant room absorption tests following standard ASTMC423 [4] for each material were made in the GAUS reverberant room (volume $= 143$ m^3). Each specimen was directly laid on the chamber floor, and its perimeter was sealed by wood framing and tape (type 'A' mounting [4]). An example for the case of ceiling tiles (that were only tested without plenum) is given in Fig. 3(a). Sabine absorption coefficients were calculated using Eq. (1).

Figure 3(b) illustrates the experiments conducted in a hemi-anechoic room following [3]. Main goal was to assess the performance of the method when applied as was described in [3]. The experimental setup was

Table 1. Measured material parameters used for simulations.

Material	Tortuosity α_∞ [-]	Porosity ϕ [-]	Resistivity σ [Nm^{-4}s]	Viscous length Λ [μm]	Thermal length Λ' [μm]	Foam mass density ρ_1 [kg.m^{-3}]
Melamine foam	1	0.98	7920	132	149	6.1
Fiberglass	1	0.99	4860	225	388	10
HDFB	1	0.96	22200	57	115	66
PU foam	2.95	0.96	9770	123	227	29.8
Tiles	> 4	0.82	> 1e6	25	60	210

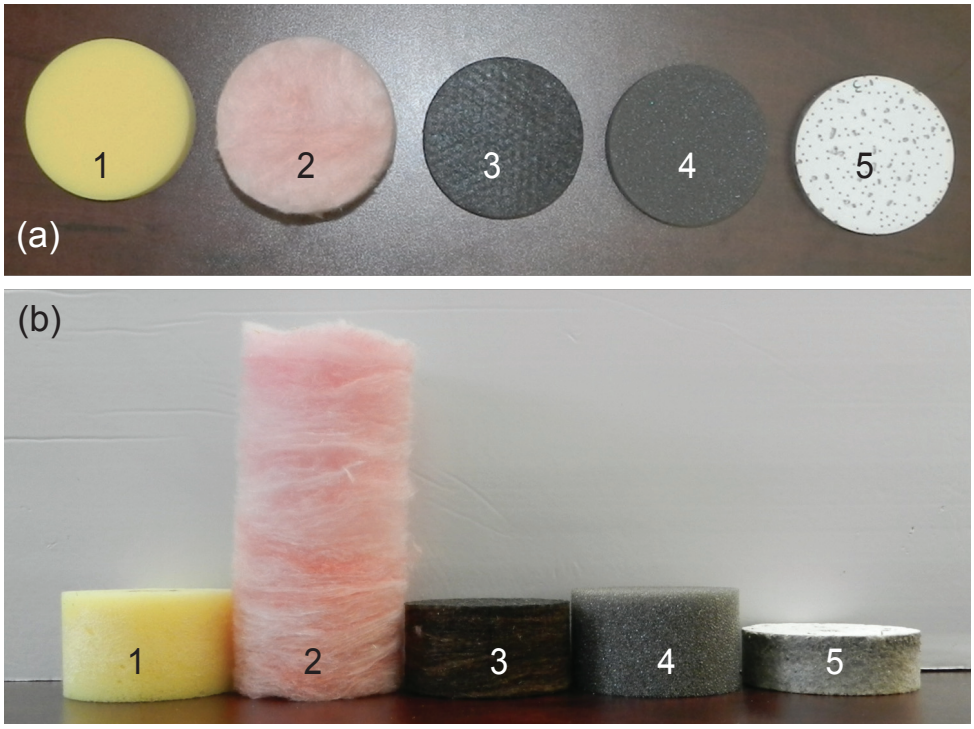

Figure 2: (a) View from top of samples of 100mm diameter used for impedance tube measurements; (b) Sideview of samples of 44.5mm diameter used for impedance tube measurements - (1) melamine foam; (2) fiberglass; (3) high density fiberglass board; (4) PU foam; (5) ceiling tile.

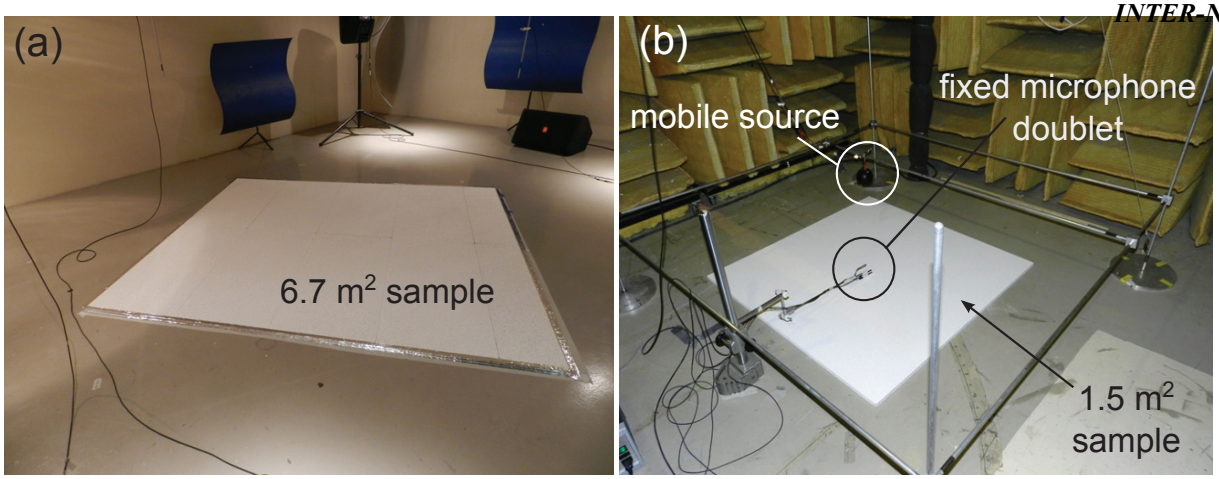

Figure 3: (a) Reverberant room measurement at GAUS laboratory – (b) Measurement under a synthetic array in a hemi-anechoic room.

nearly identical to [3], with the exception of using a small loudspeaker instead of an omnidirectional point source (leading to equivalent results, which was validated prior tests) and a swept sine instead of white noise as excitation signal in order to improve signal to noise ratio and reduce averaging time.

The specimen area was between 1.4 and 1.5 m^2 depending on the considered material. Each sample was directly laid on the chamber floor, similarly to reverberant room measurements. A small loudspeaker (Gallo Nucleus 3 in.) was manually translated using a rigid aluminium frame on a mesh of 7×7 positions above each material surface at a height $z_3 = 0.2$ m, the center source position corresponding to the normal incidence case. Each source position was separated by $\Delta_s = 0.15$ m in both x and y directions, leading to an array sidelength $L_{array} = 0.9$ m. Two microphones (BSWA $1/4$in.) were positioned at the center of samples at height $z_1 = 10$ mm and $z_2 = 60$ mm, respectively, and were amplitude calibrated only (a relative calibration operation will be used for future tests, as in [13]). The maximum incidence angle θ_{max} that can be included in the database of measured reflection coefficients $R(\theta_i, \omega)$ is defined by the source to reproduction plane separation z_s and the largest source to microphones distance, here $\theta_{max} \approx 72°$. For each source position, a logarithmic swept sine (100 Hz to 3000 Hz, in one second) was used to drive the loudspeaker, and the transfer function H between the two microphones was estimated using 15 consecutive averages. Measurements for each sample took approximately twenty minutes.

Finally, simulations based on the Transfer Matrix Method (TMM) [9] were performed. The layer of homogeneous material of infinite extent and backed by a hard wall was modeled under a limp frame assumption [9] for the melamine foam and the fiberglass, or under a rigid frame assumption for the HDFB and PUF. The ceiling tile case modeling is still under consideration, and comparison with numerical results are thus not included for this material. Since the DAF theoretically reproduced with the synthetic array implies a maximum incidence angle of $72°$, the same maximum incidence value was used as an upper bound to define the DAF excitation in all the numerical simulations presented in Section 5.

5. EXPERIMENTAL RESULTS

Figures 4(a-c) and 4(d,e) compare results obtained using the reverberant room standard measurement, the synthetic DAF measurement and simulations for an infinite material. Note that the highest frequency is voluntarily limited to the 2500 Hz third octave band since the microphone spacing of 50 mm theoretically allows for correct measurements up to a frequency of approximately 2500 Hz [5, 14].

Between frequencies of 500 and 2000 Hz and for all the materials, the Sabine coefficients values generally largely overestimate the TMM predictions, while the sound absorption values obtained using the synthetic DAF approach are in better agreement with simulations (even if the sample area was always reduced by a factor of nearly 4.5 compared with standard laboratory measurements and no specific preparation of the specimen, *i.e.* framing, was needed).

Above a frequency of 2000 Hz and depending on the considered material, the differences between simulation results and experimental results for both methods are equivalent. The microphone spacing could be

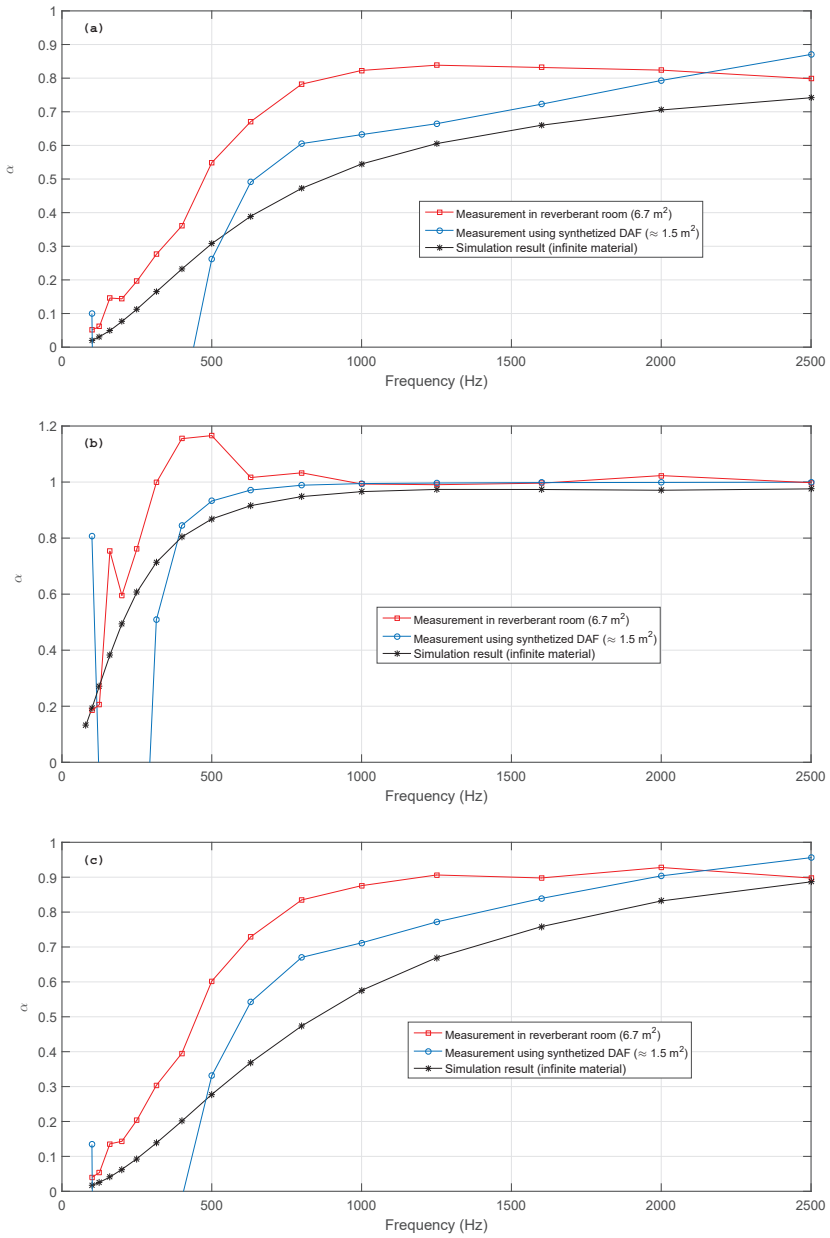

Figure 4: (a) Measurement and simulation results for the melamine foam; (b) Measurement and simulation results for the glasswool; (c) Measurement and simulation results for the high density fiberglass board.

reduced in order to improve results above this frequency for the synthetized DAF method. Note also that the fact that the measurement is made at a specific position on the material surface might explain some discrepancies with the 'global' measurement results obtained with the reverberant room method.

Below a frequency of 500 Hz, results obtained using the proposed approach are erroneous, with mostly negative values or highly overestimated sound absorption coefficient values at very low frequencies ($\approx$ 100 Hz). This is due to the use of the image source model for calculating the reflection coefficient (see Eq. 3), which leads to erroneous results when the source is placed close to the material surface, or more generally for low values of kr [5]. This can be attributed to the fact that spherical waves do not reflect only specularly, and that the simplified image source model can not be used. A more precise description of the sound field above the material is here needed especially for small source-specimen separation distance [13]. Several approaches were proposed to solve this problem, mainly in the form of iterative algorithms (see Sec.3 in [15]) based on more precise mathematical formulations such as the one of Nobile and Hayek [16]. This is one of the approaches we are currently investigating to solve this issue.

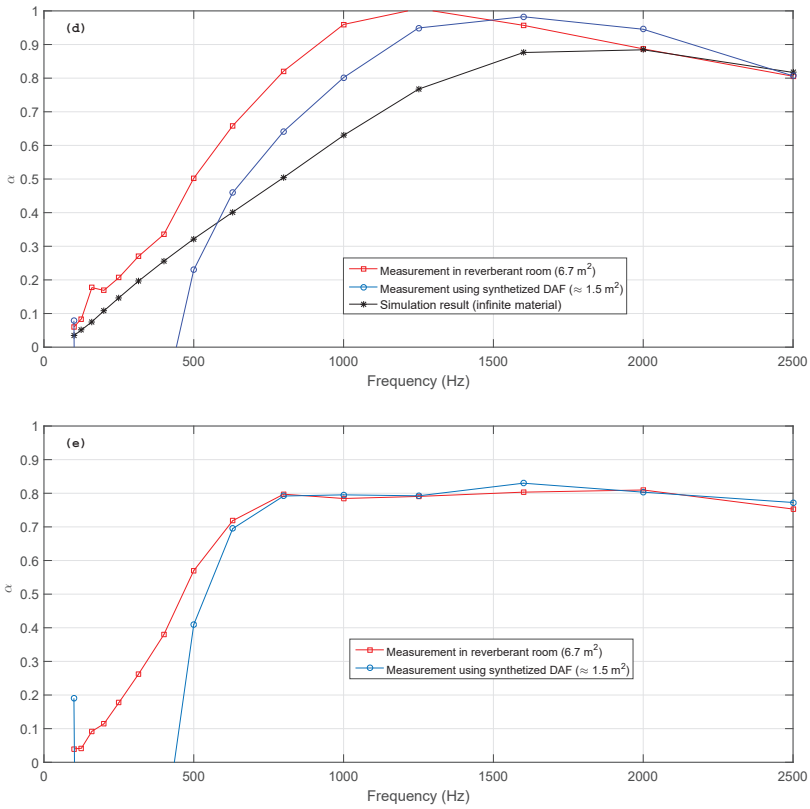

Figure 5: (d) Measurement and simulation results for the PU foam; (e) Measurement results for the ceiling tile.

6. SIMULATION RESULTS

In this section, the effect of varying the synthetic array height is studied, while keeping all the other dimensions fixed. A in-house finite element software (Novafem) is used to simulate the experimental set-up. More specifically, the complex acoustic pressures at positions z_1 and z_2 (that are similar to those used in laboratory experiments in [3]), are calculated for various monopole source heights z_3 (see fig.1(b)). These complex acoustic pressures are numerically evaluated for all source positions, the corresponding reflection coefficients are calculated using Eq. (3), and the reflection coefficient under a synthetized DAF is finally obtained using Eq. (4).

The case of a 2 in. thick melamine foam is considered, with a sidelength of 1.8 m. The synthetic array is now composed of 9×9 sources, with similar separation of 0.15 m leading to a sidelength $L_{array} = 1.2$ m. The height of the array z_3 is varied from 0.2 m to 0.8 m with a regular step of 0.2 m. Increasing the synthetic array height lowers the highest incidence angle value included in the reflection coefficients database (the two microphones being located at the vertical of the center source). The four considered source heights will correspond to cases with maximum incidence angle of 77^o, 64^o, 54^o and 46^o, respectively.

Results are shown in the upper part of Fig. 6. When the array height is increased, the sound absorption coefficients clearly decrease below a frequency of 800 Hz, while the coefficients above this frequency continuously increase. This result is the one expected when the maximum incidence angle is varied for a DAF excitation. Comparisons between simulated synthetic array and TMM simulations are given in the lower part of Fig. 6 for the lowest and the highest considered heights, with the TMM simulations using the corresponding maximum incidence angle. Above 800 Hz, the agreement between TMM and synthetic array results is very satisfactory. The larger difference observed at frequencies below 800 Hz for the largest height case is under study.

A last comparison with two experimental results obtained in [1] is finally provided. The cases of a 3×3 and 5×5 source arrays at a similar height $z_3 = 0.2$m were considered, that lead to similar maximum incidence angles for a 9×9 source array with heights 0.8 and 0.4 m (*i.e.* 46^o and 64^o). Figure 7 presents comparisons between the simulated synthetic array (with 9×9 sources and two different heights), the TMM simulation result and an experimental synthetic array (with 3×3 and 5×5 sources, and one single height),

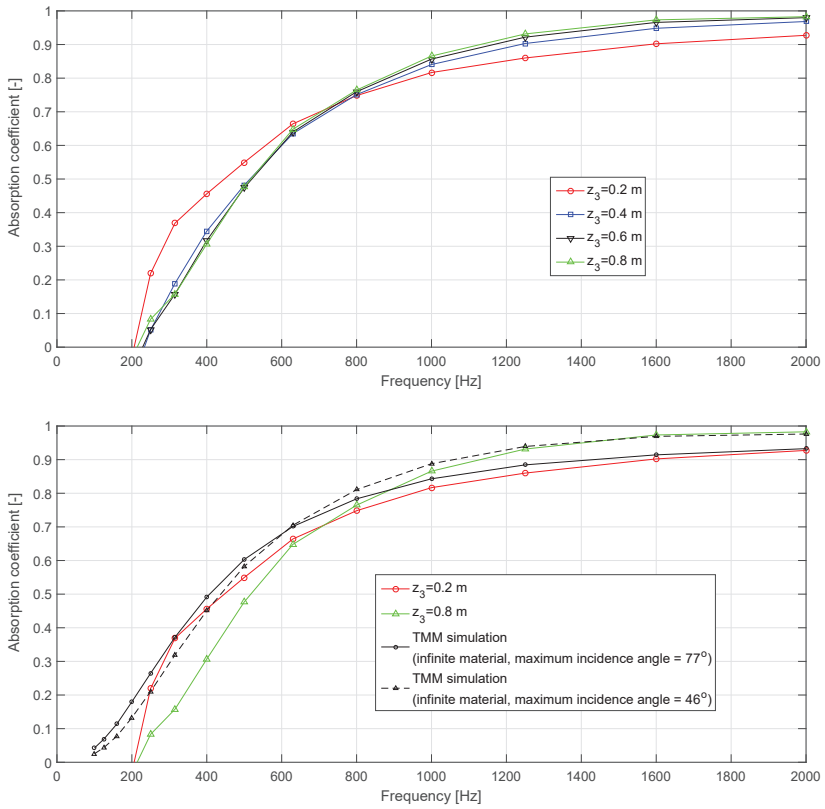

Figure 6: Upper figure : Simulation results for a 2 in.thick melamine foam, for various source heights - Lower figure : Comparison between simulation results using a synthetic array of 9×9 sources and heights $z_3 = 0.2$ m and 0.8m with TMM simulations.

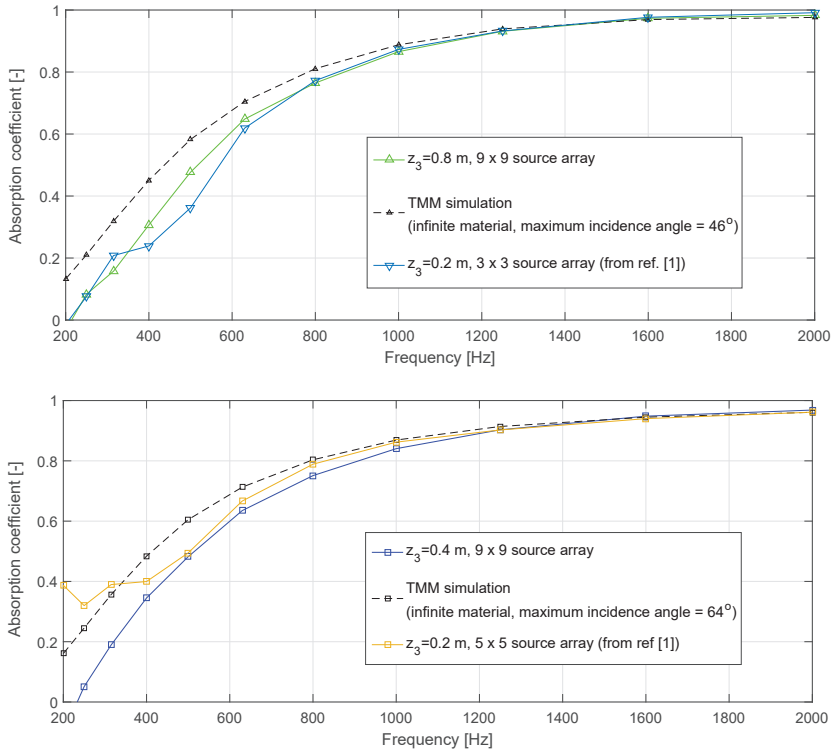

Figure 7: Comparison between simulated synthetic array, TMM simulation and experimental synthetic array – Upper figure : Case of a diffuse field with highest incidence angle of 46^o - Lower figure : Upper figure : Case of a diffuse field with highest incidence angle of 64^o.

respectively.

Interestingly, these comparisons show that for a fixed array sidelength, increasing the array height has

the same consequence as reducing the array sidelength for a fixed array height : the highest incidence angle included in the database becomes lower. This results in similar estimations of sound absorption coefficient under a DAF (thus with similar maximum incidence angle), as confirmed by results reported in Fig. 7.

7. CONCLUSION

This paper reported experimental and simulations results concerning the estimation of sound absorption coefficient using a synthetized Diffuse Acoustic Field (DAF).

It was shown that for five different acoustic materials and above the 400 Hz third octave band, the Sabine coefficients values generally largely overestimate the TMM predictions while the sound absorption values obtained using the synthetic DAF approach are in better agreement with simulations. This fact together with a reduction of the required sample size (compared with standards) makes the method attractive for laboratory measurements. Further work is nevertheless needed to fully cover the $100 - 5000$ Hz frequency range, especially in the low frequency range.

The effect of varying the source array height on the calculated sound absorption coefficient was also numerically studied for a 2 in. thick melamine foam. It was shown that increasing the array height, by limiting the highest incidence angle value inlcuded in the database of reflection coefficients, leads to similar estimations than when the sidelength of a fixed height array is reduced.

ACKNOWLEDGMENTS

This research was supported by Institut de Recherche Robert Sauvé en Santé et en Sécurité du travail.

REFERENCES

[1] O. Robin, C.-K. Amedin, A. Berry, N. Atalla, O. Doutres, and F. Sgard. Assessing sound absorption coefficient under a synthesized diffuse acoustic field: effect of the sample size and nature. In *Proceeding of 44th Interational Congress and Exposition on Noise Control Engineering (Internoise 2015): Implementing Noise Control Technology, San Francisco, CA, USA*, 2015.

[2] O. Robin, C.-K. Amedin, A. Berry, N. Atalla, O. Doutres, and F. Sgard. A numerical study of a method for estimating sound absorption coefficient under a synthesized diffuse acoustic field. In *9th International Styrian Noise, Vibration & Harshness Congress, June 22 - 24, Graz, Austria*, 2016.

[3] O. Robin, A. Berry, O. Doutres, and N. Atalla. Measurement of the absorption coefficient of sound absorbing materials under a synthesized diffuse acoustic field. *J. Acoust. Soc. Am.*, 136:EL13–EL19, 2014.

[4] ASTMC423-09a. *Standard Test Method for Sound Absorption and Sound Absorption Coefficients by the Reverberation Room Method*, ASTM International, West Conshohocken, PA, 2009.

[5] J.F. Allard and Y. Champoux. In situ two-microphone technique for the measurement of the acoustic impedance of materials. *Noise Control Engineering Journal*, 32 (1):15–23, 1989.

[6] A. Berry, R. Dia, and O. Robin. A wave field synthesis approach to reproduction of spatially-correlated sound fields. *J. Acoust. Soc. Am.*, 131(2):1226–1239, 2012.

[7] O. Robin, A. Berry, and S. Moreau. Reproduction of random pressure fields based on planar nearfield acoustic holography. *J. Acoust. Soc. Am.*, 133(6):3885–3899, 2013.

[8] B. Rafaely. Spatial-temporal correlation of a diffuse sound field. *J. Acoust. Soc. Am.*, 107:3254–3258, 2000.

[9] J.F. Allard and N. Atalla. *Propagation of Sound in Porous Media: Modelling Sound Absorbing Materials*. Wiley, Chichester, UK, 2009.

[10] O. Doutres, Y. Salissou, N. Atalla, and R. Panneton. Evaluation of the acoustic and non-acoustic properties of sound absorbing materials using a three-microphone impedance tube. *Applied Acoustics*, 71 (6):506–509, 2010.

[11] Y. Salissou and R. Panneton. Pressure/mass method to measure open porosity of porous solids. *J. Appl. Phys.*, 101:124913.1–3.7, 2007.

[12] ASTMC522-03. *Standard Test Method for Airflow Resistance of Acoustical Materials*, ASTM International, West Conshohocken, PA, 2016.

[13] J.F. Allard, Y. Champoux, and J. Nicolas. Pressure variation above a layer of absorbing material and impedance measurement at oblique incidence and low frequencies. *J. Acoust. Soc. Am.*, 86(2):766–770, 1989.

[14] Y. Champoux and A. L'Esperance. Numerical evaluation of errors associated with the measurement of acoustic impedance in a free-field using two microphones and a spectrum analyzer. *J. Acoust. Soc. Am.*, 84(1):30–38, 1988.

[15] E. Brandao, A. Lenzi, and S. Paul. A review of the in situ impedance and sound absorption measurement techniques. *Acta Acust. united Ac.*, 101:443–463, 2015.

[16] M. Nobile and S. Hayek. Acoustic propagation over an impedance plane 78, 1325-1336 (1985). *J. Acoust. Soc. Am.*, 78:1325–1336, 1985.